

Color appearance of surfaces viewed through fog

John Hagedorn, Michael D’Zmura[¶]

Department of Cognitive Sciences, University of California at Irvine, Irvine, CA 92697, USA;
e-mail: mdzmura@uci.edu

Received 15 November 1999, in revised form 27 April 2000

Abstract. How do the colors of surfaces seen through fog depend on the chromatic properties of the fog? Prior work (eg Chen and D’Zmura, 1998 *Perception* 27 595–608) shows that the colors of surfaces seen through a transparent filter can be described by a convergence model. The convergence model takes into account color shift and change in contrast. Whether the convergence model can also be applied to fog was tested experimentally with an asymmetric matching task. In computer graphic simulation, observers adjusted the color of a surface seen through fog in order to match the color of a surface seen in the absence of fog. The convergence model fits the data well. The results suggest that the color constancy revealed in this task with fog is described best by a model that takes into account both shift in color and change in contrast.

1 Introduction

Fog that lies between an observer and a surface modifies the light from the surface that reaches the eye. To light reflected from a surface is added light scattered by intervening particles. Can observers take these effects of fog into account when they judge surface color? Mahadev and Henry (1999) reported that observers can discount the increased blueness of lights from distant surfaces caused by atmospheric haze. We replicate and extend their finding of color constancy for surfaces viewed through fog in the work reported here.

Our approach originates in earlier work on color transparency. The conditions under which one perceives a gray, transparent filter that lies atop a set of surfaces were

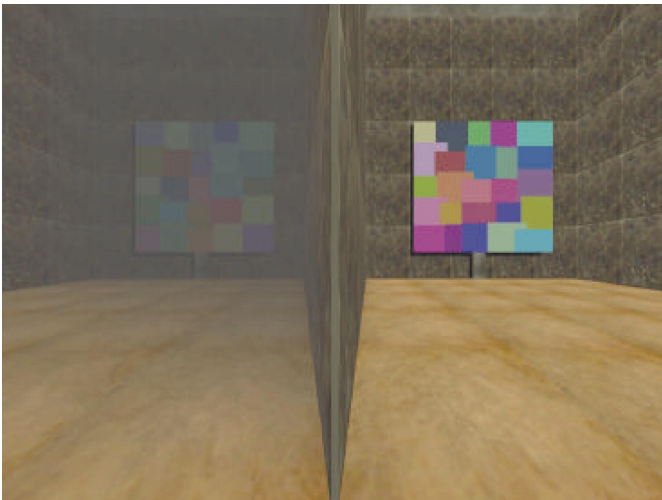


Figure 1. Stimulus configuration. This figure and figure 3 can also be seen on the *Perception* website at <http://www.perceptionweb.com/perc1000/hagedorn.html> and will be archived on the annual CD-ROM accompanying issue 12 of *Perception*.

[¶] Author to whom all correspondence and requests for reprints should be addressed.

examined systematically by Metelli (1974), Beck (1978), Gerbino et al (1990) and others. Metelli devised a model for transparency perception that involves mixing the luminance properties of overlying filter and underlying surfaces. Da Pos (1989) extended Metelli's model of transparency perception to the three dimensions of color vision by substituting tristimulus values for luminances.

This work was corroborated by observations which show that a shift in the colors of underlying surfaces or a change in their contrast can lead to transparency perception (D'Zmura et al 1997). Other systematic changes of colour, like rotations or shears in color space, do not. Furthermore, one can perceive transparency even in cases of equiluminous shifts in the colors of surfaces lying under a filter. Equiluminous color shifts are not natural. They can be generated neither by physical filters, which reduce the amount of light received from a surface, nor by devices like an episcotister (eg Heider 1932; Beck 1978), upon which Metelli's original model was based. Transparency perception in cases of equiluminous color shifts shows clearly that the study of transparency perception must be based on perception itself, rather than on particular physical instantiations.

A convergence model was proposed to take into account these observations concerning chromatic prerequisites for transparency perception (D'Zmura et al 1997; Chen and D'Zmura 1998). The model holds that an area of the visual field will appear transparent if and only if the colors of lights from surfaces along the border of the area converge towards a point in color space, as the surfaces pass from outside to within.

Do observers take into account the color shift and change in contrast caused by a transparent filter when judging surface color? The results of asymmetric color matching experiments show that they do (D'Zmura et al 2000). With the asymmetric matching technique, the color of a surface viewed under a test condition is adjusted so that it matches the color of a surface viewed under a reference condition (Wyszecki and Stiles 1982; Brainard et al 1997). Observers adjusted, in computer graphic simulation, the color of a surface seen behind a transparent filter so that it matched the color of a surface seen in plain view. The convergence model fits the color-matching data very well, suggesting that observers take into account both the color shift and the contrast change of the filter when judging surface color.

Can observers discount color shifts and changes in contrast caused by fog? Does the convergence model help to describe the color appearance of surfaces seen through fog? We use the asymmetric matching technique to answer these questions. The colors of test surfaces seen through fog are compared to the colors of reference surfaces seen in plain view. The comparison reveals the effects of fog on judgments of surface color and lets one quantify how well observers discount fog properties when judging surface color. A preliminary report of this work was made by Hagedorn and D'Zmura (1999).

2 Methods

Observers viewed two texture-mapped rooms that were positioned beside one another in computer graphic simulation (see figure 1). The two rooms were identical, with the exception that the room on the left contained fog and the room on the right did not. In each room was placed a Mondrian placard. The observer performed an asymmetric matching task by matching in colour appearance the central square of the Mondrian in the fogged room to the central square of the Mondrian in the unfogged reference room.

2.1 Display

The stimuli were presented on a Sony Trinitron GDM 20E21 color monitor, which observers viewed binocularly at a distance of 57 cm in a dark room. Software on an SGI O2 computer provided 24 bits of chromatic information for each of the 1280 × 1024 pixels presented at a field rate of 72 Hz (noninterlaced). The software corrected the nonlinear relationship between applied voltage and phosphor intensity for each gun.

Table 1. CIE 1931 standard observer chromaticity (x, y) and maximal luminance L_{\max} of each phosphor R, G, and B.

	R	G	B
x	0.621	0.286	0.150
y	0.341	0.605	0.062
$L_{\max}/\text{cd m}^{-2}$	14.6	52.6	8.28

The chromaticities and luminances of the three phosphors of the monitor were measured with a Photo Research PR-650 SpectraColorimeter and are presented in table 1.

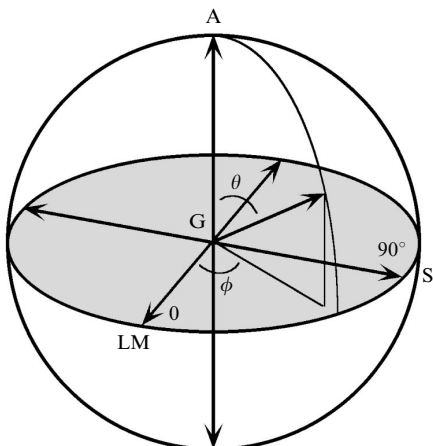
2.2 Spatial configuration

The stimulus was presented in a window that subtended $35.5 \text{ deg} \times 27.1 \text{ deg}$. Each Mondrian placard consisted of a five by five array of colored areas, each of uniform color and of approximately square shape (see figure 1). The width and height of each pseudosquare were generated randomly from a distribution uniform on the interval $[1.2, 1.8] \text{ deg}$. The square shapes were perturbed in this way in order to avoid unwanted instances of transparency that arise when squares in uniform arrays are colored randomly (D'Zmura et al 2000).

2.3 Color space

Stimulus color properties are described in the DKL color space (Derrington et al 1984), which is based on the MacLeod and Boynton (1979) color diagram (see figure 2). The neutral gray point **G** of this color space was set to the light created by displaying simultaneously each of the monitor's three phosphors at half intensity. The chromaticity of **G** was $(0.27, 0.29)$, and its luminance was 31.1 cd m^{-2} .

The color space has three axes which intersect at the gray point **G**. The first of these axes is the achromatic (A) axis, lights along which are created by generating equal modulations of the three phosphors about **G**. The other two axes lie in the equiluminous plane through **G**; lights in this plane are of equal luminance as defined by the V_λ photopic luminosity function (Wysecki and Stiles 1982). Modulation along the LM axis changes the excitations of the L and M cones and is invisible to S cones. Lights along this axis typically have a red or blue–green appearance. Modulation along the S axis changes the excitation of S cones and is invisible both to L and to M cones. Lights along the S axis typically have a purple or yellow–green appearance. Below, we specify the length of a vector that lies along a particular half axis in the DKL space in terms of cone contrast (Smith and Pokorny 1975).

**Figure 2.** DKL color space; see text for details

2.4 Chromatic properties

The pseudosquares for both the test and reference placards had R, G, and B values that were drawn randomly from a distribution uniform on the interval $[0.25, 0.75]$ (with 1.0 representing maximum possible intensity). For each pseudosquare, other than the central reference pseudosquare, an independent random draw was performed for each of the three phosphors on each trial to determine the chromatic properties of the pseudosquare.

The fog was simulated with the convergence model, the intuition for which is as follows. Suppose that the chromatic properties of the light from a surface seen in plain view are represented by a three-dimensional vector of tristimulus values \mathbf{a} . In the presence of fog, only some of the original light from the surface reaches the eye. The effects of fog can be simulated by adding some amount of a second light \mathbf{f} that depends on the chromatic properties of the fog. The resulting light \mathbf{b} that reaches the eye is a combination of the two original lights:

$$\mathbf{b} = (1 - \alpha)\mathbf{a} + \alpha\mathbf{f}, \quad (1a)$$

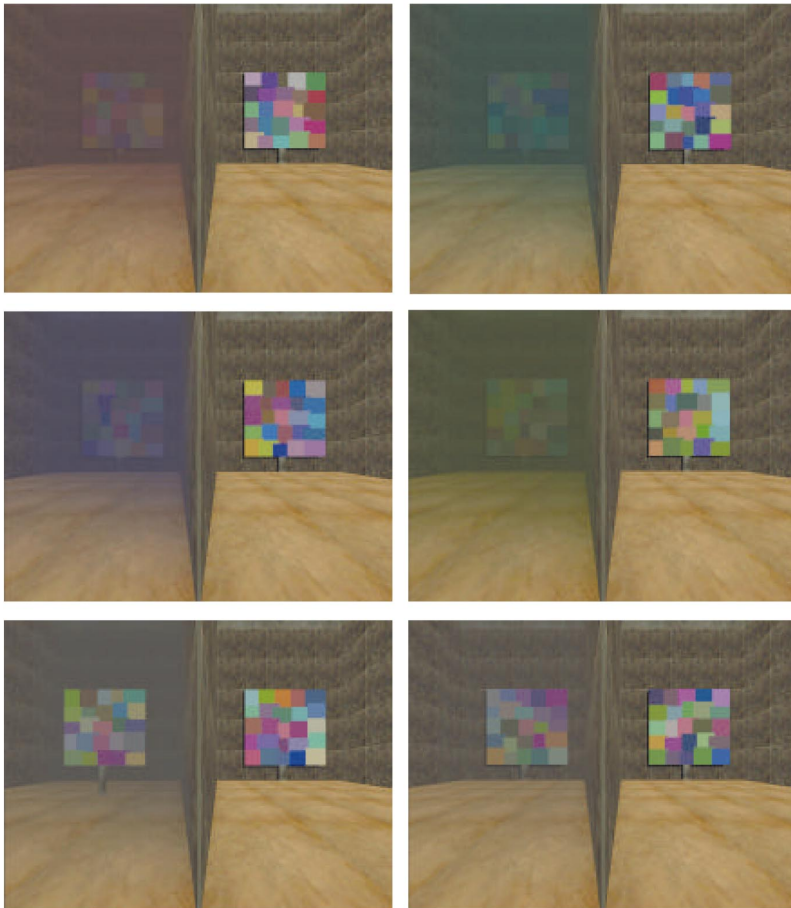


Figure 3. Various fog conditions. Four uppermost panels: full intensity fog with placard in the far position. Fog colors shown are, at upper left, ‘red’, along the positive LM half-axis; at upper right, ‘blue–green’, along the negative LM half-axis; at middle left, ‘purple’, along the positive S half-axis, and at middle right, ‘yellow–green’, along the negative S half-axis. The two lowermost panels show, at left, full-intensity gray fog with the placard in the near position; and at right, half-intensity fog with the placard in the far position.

in which the contrast reduction parameter α varies from 0 to 1 and represents the amount of fog present: no fog whatsoever ($\alpha = 0$) through fully opaque fog ($\alpha = 1$). Physical variations that can cause α to vary include fog density and viewing distance through the fog. In an equivalent formulation, one sets the translation t equal to the product αf and the contrast parameter β equal to $1 - \alpha$:

$$\mathbf{b} = \beta \mathbf{a} + t. \quad (1b)$$

The appendix presents a derivation of the convergence model from the radiative-transfer equation for light in a homogeneous scattering medium. This equation describes the chromatic and the spatial dependence of light from a surface viewed through fog (Middleton 1950; Mahadev and Henry 1999). The radiative-transfer equation can be reduced to the form of equation (1), if one assumes that the fog extinction coefficient is a constant function of wavelength. This assumption is true of natural clouds and fog that are formed from water vapor (McClatchey et al 1978). The result is a spatiochromatic convergence model [equations (A6) and (A8)], formulated in terms of tristimulus values that takes into account the distance from the observer of the viewed surface through the fog.

OpenGL graphics software was used in these experiments to display the experimental scene and to simulate the effects of fog. The OpenGL model for fog corresponds to the convergence model, formulated in terms of R, G, and B values, rather than in terms of tristimulus values (OpenGL ARB et al 1997). OpenGL graphics software allows for fog intensity to depend on fog distribution in depth in either a linear or an exponential fashion. We used fog with a linear dependence on optical depth in these experiments. We have no reason to believe that the results depend in any significant fashion on this choice.

2.5 Conditions

Fog color, fog intensity, and test placard position in depth were varied in computer graphic simulation. Twenty conditions were provided by varying factorially five fog colors, two levels of fog intensity, and two levels of placard position.

2.5.1 Fog color. Five fog colors were chosen, including gray and one for each of the four cardinal half-axes: +LM (red), -LM (blue-green), +S (purple), and -S (yellow-green). These have azimuthal angles 0° , 180° , 90° , and 270° , respectively, in the equiluminous plane of the DKL color space (figure 2). These colored fogs are shown at full intensity in the top four panels of figure 3. The RGB equivalents used in the OpenGL software for each color were gray (0.3, 0.3, 0.3), red (0.3282, 0.2360, 0.2590), blue-green (0.1531, 0.2850, 0.2573), purple (0.2645, 0.2393, 0.3510), and yellow-green (0.2169, 0.2816, 0.1653).

2.5.2 Placard position. Test placards were presented at 'far' and at 'near' levels. In a far condition, the placard was placed just in front of the back wall of the room (as shown in figure 1). A support post and a shadow on the back wall were displayed to help the observer perceive a distant placement for the placard. In the near condition, the placard was placed at a simulated distance of one-half the length of the room. As shown in the bottom two panels of figure 3, a support post was added to the placard in near position; no shadow was used. The physical size of the simulated test placard was decreased in the near conditions to keep its position on the screen and its projected size in degrees of visual angle identical to that of the placards in the far conditions. The placard in the fogless reference condition was placed in the far position.

2.5.3 Fog intensity. Fog was presented at 'full' and at 'half' intensity levels. These intensity levels correspond to choices for the contrast reduction parameter α in equations (1a) and (1b). The value of α in the half-fog conditions was 0.5, when measured for items placed in the far position, and was 0.25, when measured for items placed in

the near position. The value of α in the full-intensity fog conditions was 0.714, when measured for items in the far position, and was 0.357, when measured for items placed in the near position. One can find the corresponding values for contrast parameter β [equation (1b)] by subtracting each of the values for α from one, giving 0.5, 0.75, 0.286, and 0.643, respectively.

2.6 Observers

Three color-normal observers, two of whom (JH and MD) are authors, matched seventeen reference colors, arrayed in the equiluminous plane about the neutral gray point, for each of the twenty conditions. Reference color chromaticity coordinates are provided in table 2 and are plotted in figure 4 as filled circles. The task was to match

Table 2. CIE 1931 standard observer chromaticities of the seventeen reference stimuli. Each reference stimulus was of luminance 31.1 cd m^{-2} .

	1	2	3	4	5	6	7	8	9
x	0.2994	0.2739	0.2515	0.238	0.2406	0.267	0.3044	0.3163	0.2856
y	0.2772	0.2384	0.2296	0.2502	0.3005	0.3649	0.3877	0.3403	0.2827
	10	11	12	13	14	15	16	17	
x	0.2727	0.2602	0.2534	0.2562	0.2693	0.2853	0.2919	0.2712	
y	0.2610	0.2556	0.2679	0.2943	0.3221	0.3307	0.3122	0.2884	

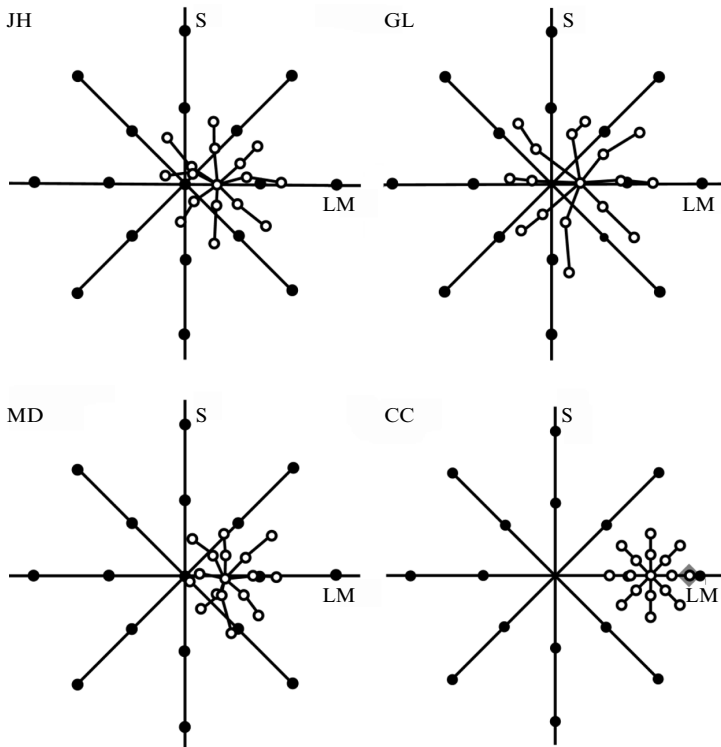


Figure 4. Results of color-matching for red fog. For each of the seventeen reference colors, shown by the filled circles, observers JH, GL, and MD made six settings whose averages are shown by the unfilled circles. The bottom right panel labeled CC shows the settings expected of a fully color-constant observer. The gray diamond in the bottom right panel along the LM axis shows the red target of convergence. Reference color chromaticities are given in table 2.

surface color appearance; observers adjusted the chromatic properties of the test square so that it appeared to be made of the same material as the reference square. Observers used the keyboard to adjust test-square appearance; six keys on the computer keyboard were arranged in three pairs to control change along the A, LM, and S axes in the DKL color space, respectively.

Observers repeated trials in just a single condition. They repeated six times the seventeen color matches made in the condition with full intensity red fog and placard at full distance. The results from this condition are shown in figure 4.

3 Results

Color-matching data were collected as a function of fog chromatic properties, fog intensity, placard position, and reference color. Five models were used in attempts to fit the data. We find that the four-parameter convergence model fits the data nearly as well as the twelve-parameter affine model, and that both provide substantially better fits than linear, translation, and von Kries scaling models. Comparing parameters found by fitting the convergence model to physical parameters of the fog used in computer graphic simulation shows varying degrees of color constancy among the three observers.

3.1 Result for red fog

The three panels labeled JH, GL, and MD in figure 4 show results for the observers in the repeated-trials condition. In this condition, the placard was placed in the far position and was viewed through fog of full intensity along the 'red' end of the LM axis. The reference colors lie in the equiluminous plane defined by the LM and S axes; these colors are indicated in the figure by filled circles. The averages of the observers' six settings per reference color are shown by the open circles.

Neither a shift of the reference colors toward the 'red' end of the LM axis, nor a convergence of the reference colors toward the neutral gray point at the center of the diagram, describes the data. Simultaneous color shift and contrast reduction are required to help model perceived surface color in this task.

Were observers to discount fully the chromatic transformation caused by the fog, then their settings would be like those marked CC ('color constant') in the bottom right panel of figure 4. The color constant settings lie closer to the target of convergence [f in equation (1a)] marked by the gray diamond, than do the settings of the observers. This indicates that observers take the color shift caused by the fog only partially into account when judging surface color. In addition, the color-constant settings lie closer to one another than do the observers' settings. This indicates that the observers take the reduction of contrast caused by the fog only partially into account. The plots show also that observer GL makes color-matching settings that are less 'color-constant'; GL's settings show smaller effects of color shift and contrast reduction caused by the fog. This point is amplified below in section 3.4.

3.2 Model fitting

We fit the data from the twenty conditions using affine, convergence, linear, translation, and von Kries scaling models. Linear regression was used to minimize the residual mean squared error between the A, LM, and S axis coordinates of model predictions and the coordinates of observers' actual settings. Distance between two colors is measured in a version of the DKL color space (Derrington et al 1984) that is scaled so that one unit along A, LM, or S axes corresponds approximately to threshold. Contrast sensitivities of 200, 1000 for L-cones, and 100 for S-cones were used along A, LM, and S axes, respectively. These sensitivities correspond to (reciprocal) threshold contrasts of 0.005 along the A axis, 0.001 to L cones along the LM axis, and 0.01 to S cones along the S axis, respectively (Lennie and D'Zmura 1988).

Five models were fit to the data: affine, convergence, linear, translation, and von Kries scaling. The affine model is described by the equation

$$\mathbf{b} = \mathbf{M}\mathbf{a} + \mathbf{t}, \quad (2)$$

in which \mathbf{a} is a three-dimensional vector of reference color coordinates, \mathbf{M} is a 3×3 matrix describing a linear transformation, \mathbf{t} is a three-dimensional translation vector, and \mathbf{b} is a predicted vector of test color coordinates (Jameson and Hurvich 1964; Brainard et al 1997). When fitting the model to the color-matching data found by an observer in a particular condition, one chooses the entries of the matrix \mathbf{M} and the vector \mathbf{t} so as to minimize the RMS error between the predictions and an observer's actual settings. The affine model has twelve parameters that may be adjusted during the fitting procedure: nine for the 3×3 linear transformation \mathbf{M} and three for the color shift \mathbf{t} .

The convergence model [equation (1b)] is a special case of the affine model with only four parameters. The linear model, too, is a special case of the affine model and is formulated by removing the translation \mathbf{t} from equation (2):

$$\mathbf{b} = \mathbf{M}\mathbf{a}. \quad (3)$$

Likewise, the translation model is a special case found by removing the linear transformation \mathbf{M} from equation (2):

$$\mathbf{b} = \mathbf{a} + \mathbf{t}. \quad (4)$$

The von Kries (1905) scaling model, finally, can be expressed by the equation

$$\mathbf{b}' = \mathbf{D}\mathbf{a}', \quad (5)$$

in which \mathbf{a}' is a vector of reference color L-, M-, and S-cone excitations, and \mathbf{D} is a diagonal matrix that scales the cone excitations to produce the cone excitations \mathbf{b}' predicted by the model. To fit data with this model, color specifications in the DKL space are first converted into the LMS space of cone excitations. One then attempts to fit the data using three factors to scale the respective cone excitations. The results are then converted from the LMS space back to the DKL space so that they may be compared with the fits of the other models.

3.3 Model fits

Figure 5 shows the sum of residual mean squared errors for the three observers JH, MD, and GL. The models are indicated below the horizontal axis by their first letter: A—affine, C—convergence, L—linear, T—translation, and S—von Kries scaling. Better fits correspond to smaller residual error values.

The affine model (leftmost columns) fits the data best; indeed, the affine model must perform at least as well as the other models, because the others are all instances

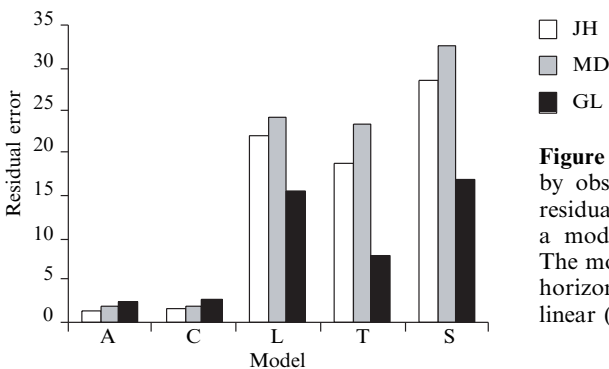


Figure 5. Model fits for the color conditions, by observer. Each column lists the sum of residual mean squared errors found in fitting a model to each of the twenty conditions. The model is listed by its first letter along the horizontal axis: affine (A), convergence (C), linear (L), translation (T), scaling (S).

of it. The results show also that the convergence model fits the data nearly as well as the affine model, and that the other three models fit the data less well. The similarity in the abilities of the affine and convergence models to fit the data suggests that the eight extra degrees of freedom within the linear transformation of the affine model do not account for much variance in the data beyond that accounted for by the contrast-reduction parameter. Note also that the fits to GL's data by the linear, translation, and scaling models are better than the fits to the data of JH and MD by these models.

Figure 6 shows that there is no significant dependence of the quality of fits on fog color.

The effect of fog intensity on the model fits are shown in figure 7. Again, the affine and convergence models fit the data substantially better than the linear, translation, and scaling models. The affine and convergence model fits are slightly better in the full-intensity fog conditions than in the half-intensity fog conditions. The other models—linear, translation, and scaling—fail to fit the data, especially in the full-intensity conditions.

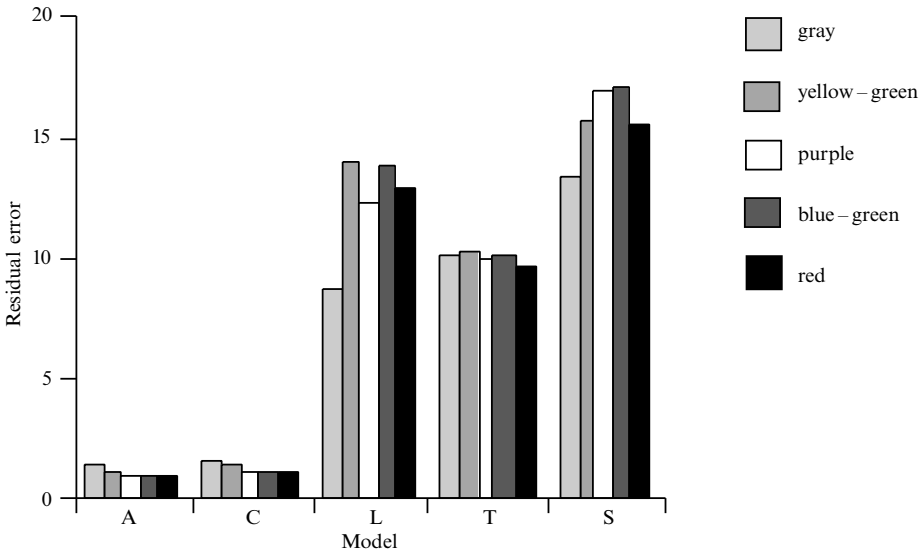


Figure 6. Fog color has little effect on model fits. Each column lists the sum of residual mean squared errors found in each of four conditions per color, averaged across the three observers. Model labels are as in figure 5.

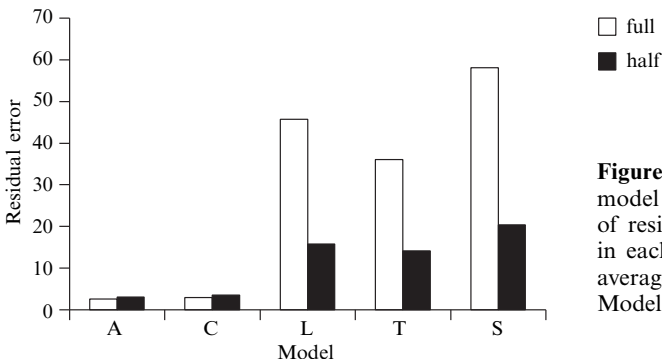


Figure 7. Effects of fog intensity on model fits. Each column lists the sum of residual mean squared errors found in each of ten conditions per intensity, averaged across the three observers. Model labels are as in figure 5.

Figure 8 shows the effects of placard position on the model fits. The affine and convergence models fit the data well, and perform slightly better for the far-placard conditions than for the near-placard positions. The linear, translation, and von Kries models fit the data less well, but perform better for the near-placard condition.

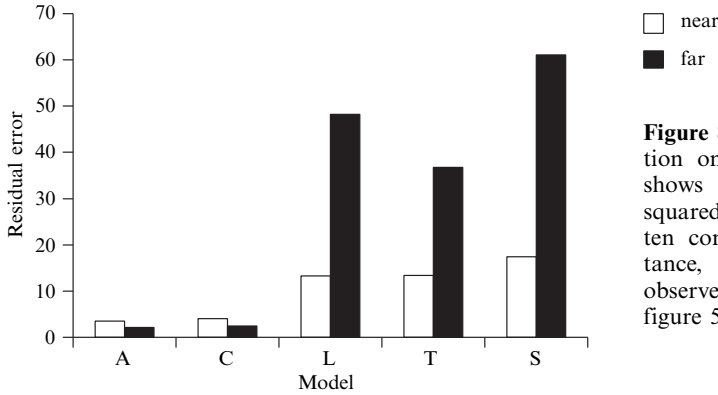


Figure 8. Effects of placard position on model fits. Each column shows the sum of residual mean squared errors found in each of ten conditions per simulated distance, averaged across the three observers. Model labels are as in figure 5.

The results for fog intensity and for placard position shown in figures 7 and 8, respectively, indicate that the affine and convergence models fit the color-matching data better in conditions with relatively more intervening fog, as in the full-intensity and far-placard conditions. Conversely, the linear, translation, and von Kries models perform better in conditions with relatively less intervening fog. The affine and convergence models fit best in all conditions.

3.4 Color constancy results

One can use the fits to data provided by the convergence model to estimate the degree of color constancy exhibited by each observer at each condition. The fits provide estimates of the scalar contrast parameter $\hat{\beta}$ and the vector color shift parameter \hat{t} [equation (2)] required for the fit by the convergence model.

Figure 9 shows scatter plots, for each observer, of the estimates $\hat{\beta}$ of perceived contrast versus the actual values β required to generate the fogs in the various experimental conditions. Each point in the plot represents a pair of perceived and actual contrast values, found for each observer and for each condition. The Pearson product moment correlation coefficients for each observer are given in table 3. Perceived and actual contrast are highly correlated; the correlation coefficients range from 0.94 to 0.96.

The best-fit lines have slopes 0.80 (GL), 1.01 (MD), and 1.14 (JH), while the intercepts are 0.34 (GL), -0.06 (MD), and -0.06 (JH). The intercepts are of negligible value, with the exception of that for observer GL. The two observers JH and MD evidently take the contrast properties of fog into account fully when judging surface color. There is a

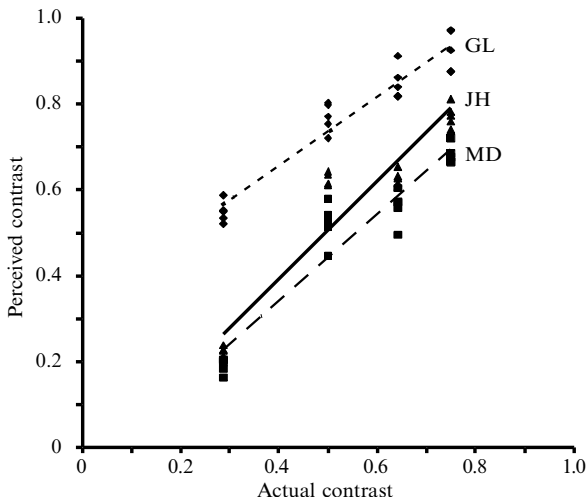


Figure 9. Plot of perceived contrast versus actual contrast for observers GL (diamonds), JH (triangles), and MD (squares). Estimates $\hat{\beta}$ of the contrast parameters for each observer for each condition, found by fitting the convergence model to observers' data, are plotted against the actual, physical contrasts β of the fogs simulated in corresponding conditions. Parameters of the best-fit lines are given in table 3.

Table 3. Correlation between the estimates $\hat{\beta}$ found by fitting the convergence model to the data of observers JH, MD, and GL and the actual contrast reduction β of the fogs used in the twenty experimental conditions. Shown are Pearson product moment correlations, as well as the slopes and intercepts of best-fitting lines (pictured in figure 9).

	JH	MD	GL
Correlation	0.942	0.955	0.963
Slope	1.138	1.013	0.800
Intercept	-0.061	-0.064	0.337

nearly one-to-one correspondence between the contrast estimates $\hat{\beta}$ and the actual values β for observers JH and MD. While the slope for observer GL is also high, this is offset by the high value of the intercept, so that the estimates of perceived contrast $\hat{\beta}$ are uniformly higher than the actual values. Higher values indicate that reduction of contrast by fog is not taken fully into account by GL. Recall that the parameter β of the convergence model [equation (1b)] reports surface contrast: a value of 1 for β corresponds to no reduction in the contrast of the surface, while a value of 0 corresponds to a total reduction in contrast. The higher estimates $\hat{\beta}$ for GL thus correspond to smaller estimates of perceived contrast reduction.

In figure 10 are shown scatter plots of estimated and actual lengths of color shift vectors. Each point represents an estimate of the length of the perceived color shift found by fitting the convergence model to an observer's data in an experimental condition (vertical axis) and the actual length (horizontal axis). Table 4 shows the correlation

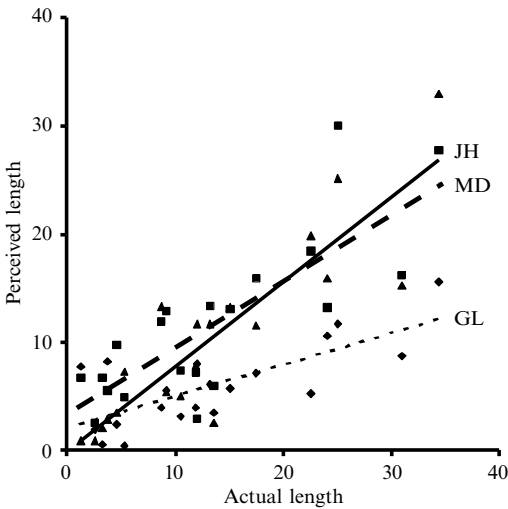


Figure 10. Plot of magnitude of perceived color shift versus magnitude of actual color shift for observers GL (diamonds), JH (triangles), and MD (squares). Estimates of the lengths of the perceived color shifts \hat{t} for each observer for each condition, found by fitting the convergence model to observers' data, are plotted against the lengths of the actual color shifts t of the fogs simulated in corresponding conditions. Parameters of the best-fit lines are given in table 4.

Table 4. Correlation between the lengths of perceived color shifts \hat{t} fit to the data of observers JH, MD, and GL, and the lengths of actual color shifts t . Shown are Pearson product moment correlations, as well as the slopes and intercepts of best-fitting lines (pictured in figure 10). The intercepts are shown in threshold-scaled units.

	JH	MD	GL
Correlation	0.778	0.555	0.607
Slope	0.780	0.623	0.292
Intercept	-0.133	3.171	2.002

coefficients for each observer. They range from 0.56 to 0.78 and, although less high in value than those for contrast reduction, they are significant. The slopes and intercepts of the best-fit lines are given in table 4 also. The intercepts, which are reported in threshold-scaled units, are negligible in value. The slopes for MD and JH are 0.62 and 0.78, respectively, while that for GL is 0.29. These slopes suggest that the first two observers take between 60%–80% of the actual color shift into account when judging surface color. The third observer, GL, takes about 30% of the shift into account, so evincing less color constancy, which agrees with the perceived contrast results found for this observer.

The azimuthal angles of perceived color shifts within the equiluminous plane are compared to the azimuthal angles of the actual color shifts in figure 11. Actual azimuthal angles of the fog stimuli were 0° for +LM ('red'), 90° for +S ('purple'), 180° for -LM ('blue-green'), and 270° for -S ('yellow-green'). The correlations for the three observers are uniformly very high (see table 5). The plot shows that observers made settings that, for the most part, agreed very closely with the actual azimuths. The points in the plot lie close to the diagonal line, which has a slope of 1 and an intercept of 0.

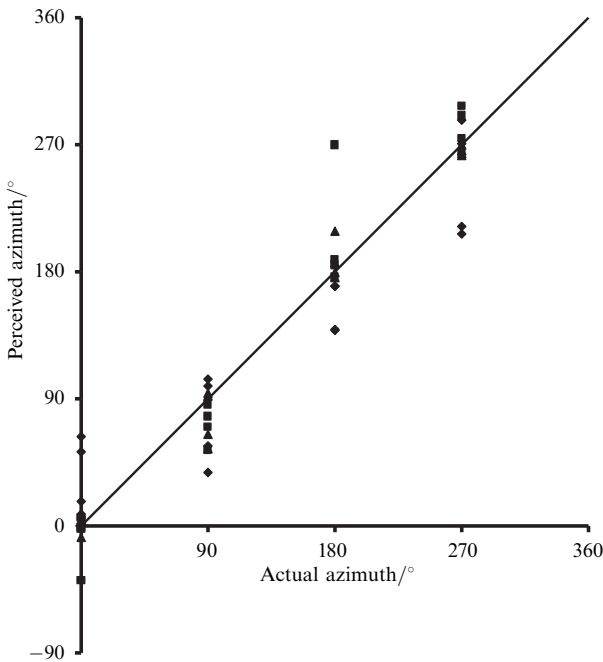


Figure 11. Plot of azimuthal angle of perceived color shift versus azimuthal angle of actual color shift for observers GL (diamonds), JH (triangles), and MD (squares). Estimates of the azimuthal angles, within the equiluminous plane, of the perceived color shifts \hat{t} for each observer for each condition are plotted against the azimuthal angles of the actual color shifts t . Actual azimuthal angles were 0° (+LM, 'red'), 90° (+S, 'purple'), 180° (-LM, 'blue-green') and 270° (-S, 'yellow-green'). The diagonal line has slope 1 and intercept 0.

Table 5. Correlation between the azimuthal angles in the equiluminant plane of color shifts \hat{t} fit to the data of observers JH, MD, and GL, and the azimuthal angles of fog actual color shifts t .

	JH	MD	GL
Correlation	0.991	0.975	0.937

4 Discussion

The results of these asymmetric color-matching experiments show that observers take into account the chromatic properties of fog when judging surface color. Observers discount two aspects of the chromatic properties of fog: reduction in contrast and shift in the colors of lights from surfaces. Two of the observers in this study discounted contrast reduction fully, and discounted somewhere between 60%–80% of the color

shift. These two observers—the authors—exhibit nearly complete color constancy. The other, naïve, observer, discounted contrast reduction and color shift only partially.

In all cases, the convergence model fit the data nearly as well as the affine model, even though the affine model has twelve parameters and the convergence model has only four. Linear, translation, and von Kries scaling models fit the data considerably less well in all cases. That the asymmetric color-matching data are fit well by the convergence model suggests that observers take into account both contrast reduction and shift in color when judging the colors of surfaces seen through fog.

It may seem tautological to test a convergence model of visual processing with fog stimuli that are modeled in the same way. Yet it need not have been the case that the visual system takes fog contrast reduction and color shift into account when judging surface color. For instance, were our visual systems unable to take into account fog contrast reduction, then translation and von Kries scaling models would have done just as well in fitting the data as the more general convergence and affine models. Yet the results of the present experiments show convincingly that observers do take contrast variation into account when judging surface color.

A similar result was found in recent experiments on the colors of surfaces seen to lie behind a transparent filter (D’Zmura et al 2000). Observers took into account both contrast reduction and color shift caused by such a filter. Asymmetric color matches showed that approximately one-half of the reduction of contrast and one-half of the color shift caused by a transparent filter were taken into account by the observers. Again, the convergence model fit the data nearly as well as the affine model and performed substantially better than linear, translation, or von Kries scaling models.

Fog differs from a transparent filter in two ways. First, the chromatic effects of fog increase with depth, as the amount of fog intervening between surface and viewer increases. Unlike a transparent filter, fog imposes a chromatic transformation on underlying surfaces that depends strongly on the depth of a surface behind the filter. Second, fog tends to have poorly defined borders, while transparent filters tend to have clearly-demarcated borders defined by sharp edges and X-junctions (Heider 1932).

Common to both fog and a transparent filter are the scission or perceived layering in depth of the visual field into chromatic processes (Faul 1997; Mausfeld 1998). The layers include opaque surfaces, seen to lie farther away from the observer, and intervening chromatic processes like illumination, transparency, and fog. Our results with transparency and with fog suggest that the convergence model describes the color appearance of surfaces in cases of scission (D’Zmura et al, in press). Observers can discount both shift in color and change in contrast caused by an intervening color process.

Observers match color in these experiments by finding the color for the test surface, seen through an intervening color process, that causes it to appear to be made of the same stuff as the reference surface. Such a ‘paper’ or surface-color match differs from a ‘colorimetric’ match, for which one attempts to set the color of the test area so that it matches the color of the reference area, independently of context provided by surrounding elements (Arend and Reeves 1986). The two situations that are compared by observers in experiments with fog and with transparency involve highly visible color differences.

That we are able to take into account changes in contrast when judging surface color was first pointed out by Brown and MacLeod (1992). There are two potential ways in which such a compensation may be done. The first is an automatic contrast gain control, which is known to operate within both achromatic and color-opponent channels [see review by D’Zmura and Singer (1999)]. This automatic compensation has been studied by colorimetric matches. The second is through a conscious judgment concerning visible processes; this has been studied here with surface-color matches.

Acknowledgements. We thank an anonymous referee for help in clarifying the relationship between the Beer–Lambert law and the radiative transfer equation. This work was supported by NIH EY10014 and by NSF DB9724595.

References

- Arend L E, Reeves A, 1986 “Simultaneous color constancy” *Journal of the Optical Society of America A* **3** 1743–1751
- Beck J, 1978 “Additive and subtractive color mixture in color transparency” *Perception & Psychophysics* **23** 265–267
- Brainard D H, Brunt W A, Speigle J M, 1997 “Color constancy in the nearly natural image. 1. Asymmetric matches” *Journal of the Optical Society of America A* **14** 2091–2110
- Brown R O, MacLeod D I A, 1992 “Saturation and color constancy”, in *Advances in Color Vision Technical Digest* (Washington, DC: Optical Society of America) pp 110–111
- Chen V J, D'Zmura M, 1998 “Test of a convergence model for color transparency perception” *Perception* **27** 595–608
- Da Pos O, 1989 *Transparenze* (Padua: Icone)
- Derrington A M, Krauskopf J, Lennie P, 1984 “Chromatic mechanisms in lateral geniculate nucleus of macaque” *Journal of Physiology (London)* **357** 241–265
- D'Zmura M, Colantoni P, Hagedorn H, in press “Perception of color change” *Color Research and Application*
- D'Zmura M, Colantoni P, Knoblauch K, Laget B, 1997 “Color transparency” *Perception* **26** 471–492
- D'Zmura M, Rinner O, Gegenfurtner K R, 2000 “The colors seen behind transparent filters” *Perception* **29** 911–926
- D'Zmura M, Singer B, 1999 “Contrast gain control”, in *Colour Vision: From Genes to Perception* Eds L T Sharpe, K R Gegenfurtner (Cambridge: Cambridge University Press) pp 369–385
- Faul F, 1997 “Theoretische und experimentelle Untersuchung chromatischer Determinanten perzeptueller Transparenz”, Dissertation, Christian-Albrechts-Universität zu Kiel, Kiel, Germany
- Gerbino W, Stultiens C I F H J, Troost J M, Weert C M M de, 1990 “Transparent layer constancy” *Journal of Experimental Psychology: Human Perception and Performance* **16** 3–20
- Hagedorn J B, D'Zmura M, 1999 “Color appearance of surfaces viewed through fog” *Investigative Ophthalmology & Visual Science* **40**(4) S750
- Heider G M, 1932 “New studies in transparency, form and color” *Psychologische Forschung* **14** 13–55
- Jameson D, Hurvich L M, 1964 “Theory of brightness and color contrast in human vision” *Vision Research* **4** 135–154
- Kries J von, 1905 “Die Gesichtsempfindungen”, in *Handbuch der Physiologie des Menschen* volume 3 Ed. W Nagel (Braunschweig: Vieweg) pp 109–279
- Lennie P, D'Zmura M, 1988 “Mechanisms of color vision” *Critical Reviews in Neurobiology* **3** 333–400
- McClatchey R A, Fenn R W, Selby J E A, Volz F E, Garing J S, 1978 “Optical properties of the atmosphere”, in *Handbook of Optics* Ed. W G Driscoll (New York: McGraw-Hill) pp 14.1–14.65
- MacLeod D I A, Boynton R M, 1979 “Chromaticity diagram showing cone excitation by stimuli of equal luminance” *Journal of the Optical Society of America* **69** 1183–1186
- Mahadev S, Henry R C, 1999 “Application of a color-appearance model to vision through atmospheric haze” *Color Research and Application* **24** 112–120
- Mausfeld R, 1998 “Color perception: From Grassmann codes to a dual code for object and illuminant colors”, in *Color Vision* Eds W Backhaus, R Kliegl, J Werner (Berlin: deGruyter) pp 219–250
- Metelli F, 1974 “The perception of transparency” *Scientific American* **230**(4) 91–98
- Middleton W E K, 1950 “The colors of distant objects” *Journal of the Optical Society of America* **40** 373–376
- OpenGL ARB, Woo M, Neider J, Davis T, 1997 *OpenGL Programming Guide* second edition (New York: Addison-Wesley)
- Smith V C, Pokorny J, 1975 “Spectral sensitivity of the foveal cone photopigments between 400 and 500 nm” *Vision Research* **15** 161–171
- Wyszecki G, Stiles W S, 1982 *Color Science. Concepts and Methods, Quantitative Data and Formulae* (New York: John Wiley)

Appendix. A spatiochromatic convergence model

The radiative transfer equation for light through a homogeneous medium can be used to describe the spatial and chromatic dependence of light from a surface viewed through fog. The radiative transfer equation can be reduced to the form of the convergence model, if one assumes that the fog extinction coefficient is a constant function of wavelength. This assumption holds true of natural clouds and fog, formed from water vapor (McClatchey et al 1978). The result is a formulation of the convergence model, in terms of cone tristimulus values, that takes into account the distance from the observer of the viewed surface through the fog.

The radiative transfer equation for light, assuming a horizontal sight path in a homogeneous scattering medium, is given by the following equation (Middleton 1950; Mahadev and Henry 1999):

$$L(x, \lambda) = S(\lambda) \exp[-\tau(x, \lambda)] + \left[\frac{h(\lambda)}{\varepsilon(\lambda)} \right] \{1 - \exp[-\tau(x, \lambda)]\}. \quad (\text{A1})$$

In this equation, $L(x, \lambda)$ is the radiance of the light reaching the eye and $S(\lambda)$ is the radiance of the light from the surface prior to its passage through the fog. The variable x refers to the distance of the viewed surface through uniform fog, and λ refers to visible wavelength. The function of wavelength $\varepsilon(\lambda)$ in equation (A1) is the extinction coefficient of the fog, and $\tau(x, \lambda)$ is the optical depth of the viewed surface and is related to the extinction coefficient by

$$\tau(x, \lambda) = \varepsilon(\lambda)x. \quad (\text{A2})$$

The function $h(\lambda)$, finally, describes the light from the air along the line of sight and quantifies scattered light per unit length and volume of fog.

The first term on the right-hand side of equation (A1) describes the light transmitted from the surface to the viewer through the fog. It represents the integral form of the Beer–Lambert law, on the assumption of a homogeneous medium. The second term describes the path radiance, or light that reaches the viewer from the fog that did not originate from the surface.

If one assumes that the extinction coefficient $\varepsilon(\lambda)$ is a constant function ε of wavelength, then the optical depth may be expressed simply as a function of distance:

$$\tau(x, \lambda) = \tau(x) = \varepsilon x. \quad (\text{A3})$$

The three tristimulus values q_1, q_2, q_3 of the light with radiance $L(x, \lambda)$ can be determined by integrating the product of the radiance and each of the three spectral sensitivity functions $Q_i(\lambda)$, $1 \leq i \leq 3$:

$$q_i(x) = \langle Q_i(\lambda), L(x, \lambda) \rangle, \quad 1 \leq i \leq 3, \quad (\text{A4})$$

in which $\langle j, k \rangle$ is used as a shorthand for the integral over the visible spectrum of the product of two functions of wavelength j and k . Substituting the right-hand side of equation (A1) for the radiance in equation (A4) and assuming that equation (A3) holds true, one finds that

$$q_i(x) = \langle Q_i(\lambda), S(\lambda) \rangle \exp(-\varepsilon x) + \left\langle Q_i(\lambda), \frac{h(\lambda)}{\varepsilon} \right\rangle [1 - \exp(-\varepsilon x)], \quad (\text{A5})$$

or

$$q_i(x) = \exp(-\varepsilon x)a_i + [1 - \exp(-\varepsilon x)]f_i, \quad \text{for } 1 \leq i \leq 3, \quad (\text{A6})$$

where

$$a_i = \langle Q_i(\lambda), S(\lambda) \rangle \quad (\text{A7a})$$

and

$$f_i = \left\langle Q_i(\lambda), \frac{h(\lambda)}{\varepsilon} \right\rangle, 1 \leq i \leq 3. \quad (\text{A7b})$$

Equation (A6) has the form of the convergence model but specifies the spatial dependence of the tristimulus values.

The integrals in equation (A5) would not separate nicely were the extinction coefficient to depend on wavelength. In that case, the optical depth τ would depend on wavelength and would remain inside the integral with the spectral sensitivity function (Middleton 1950). The assumption of a constant extinction coefficient allows one to separate spatial from spectral forms in the radiative transfer equation to provide a spatiochromatic convergence model [equation (A6)].

A simple generalization lets one model a non-exponential fall-off of contrast with increasing optical depth, of the sort that might arise with fog of space-varying density. Substituting the fall-off function $d(x)$ for $\exp(-\varepsilon x)$ in equation (A6) produces the following, more general, formulation:

$$q_i(x) = d(x)a_i + [1 - d(x)]f_i, 1 \leq i \leq 3. \quad (\text{A8})$$

One uses a fall-off function $d(x)$ which is a monotonic decreasing function of distance x with range $[0, 1]$.